

# Organic & Biomolecular Chemistry

Accepted Manuscript



This is an *Accepted Manuscript*, which has been through the Royal Society of Chemistry peer review process and has been accepted for publication.

*Accepted Manuscripts* are published online shortly after acceptance, before technical editing, formatting and proof reading. Using this free service, authors can make their results available to the community, in citable form, before we publish the edited article. We will replace this *Accepted Manuscript* with the edited and formatted *Advance Article* as soon as it is available.

You can find more information about *Accepted Manuscripts* in the [Information for Authors](#).

Please note that technical editing may introduce minor changes to the text and/or graphics, which may alter content. The journal's standard [Terms & Conditions](#) and the [Ethical guidelines](#) still apply. In no event shall the Royal Society of Chemistry be held responsible for any errors or omissions in this *Accepted Manuscript* or any consequences arising from the use of any information it contains.

## $\gamma$ -CYCLODEXTRIN MODULATES CHEMICAL REACTIVITY BY MULTIPLE COMPLEXATION

J. Fernández-Rosas<sup>a</sup>, M. Pessêgo<sup>a, b</sup>, M. Cepeda<sup>c</sup>, N. Basilio<sup>d</sup>, M. Parajó<sup>a</sup>, P. Rodríguez-Dafonte<sup>a</sup>, L. García-Río<sup>\*a</sup>

<sup>a</sup>Departamento de Química Física, Centro de Investigación en Química Biológica y Materiales Moleculares (CIQUS), Universidad de Santiago, 15782 Santiago, Spain.

<sup>b</sup>CIQA, Departamento de Química e Farmácia, Faculdade de Ciências e Tecnologia, Universidade do Algarve, Campus de Gambelas, 8005-139 Faro, Portugal.

<sup>c</sup>Departamento de Química, Universidad Andrés Bello, Av. República 275, Santiago, Chile.

<sup>d</sup>REQUIMTE, Departamento de Química, Faculdade de Ciências e Tecnologia, Universidade Nova de Lisboa, 2829-516 Caparica, Portugal.

### ABSTRACT

Multiple complexation by  $\gamma$ -CD has been studied by self-diffusion coefficients (DOSY) and chemical kinetics experiments in which 4-methoxybenzenesulfonyl chloride (MBSC) solvolysis was used as a chemical probe. The addition of surfactant as a third component to the reaction mixture induced a very complex reactivity pattern that was explained on the basis of multiple complexation phenomena and surfactant self-assembly to form micelles. A cooperative effect that yielded a ternary complex formed by cyclodextrin-surfactant-MBSC was observed. The larger cavity of  $\gamma$ -CD in comparison with  $\beta$ -CD is responsible for the change from the competitive complexation mechanism predominant with  $\beta$ -CD to a cooperative/competitive mixed mechanism operating for the larger derivative. The cavity size in  $\gamma$ -CD is large enough to bind two surfactant alkyl chains with a cooperative effect. Water molecules released by the formation of 1:1 host/guest complexes made the cavity more hydrophobic and promoted further inclusion. A reduction in the available volume of the cavity should be considered on binding a second guest.

## INTRODUCTION

Cyclodextrins (CDs) are cyclic oligosaccharides composed of D-glucopyranose units linked by  $\alpha(1\rightarrow4)$  bonds to give units that are shaped like a truncated cone with a hydrophobic cavity<sup>1</sup>. Commercially available  $\alpha$ ,  $\beta$ , and  $\gamma$ -CDs have six, seven, and eight D-glucopyranose units, respectively. CDs have a relatively hydrophobic cavity and, as a consequence, an organic molecule with appropriate dimensions can be incorporated into the CD cavity to form an inclusion complex. The driving force for native CDs to bind organic guests has been discussed in terms of hydrophobic and van der Waals interactions, hydrogen bonding, the release of high energy water molecules, and steric strain – all effects that are often not sufficient to achieve strong and selective complexation<sup>1,2</sup>. Multiple sites and modes of interaction are prerequisites to improve the binding affinity and manipulate the arrangement of guest molecules within the CD cavity.

Host:guest interactions involving CDs and small organic molecules predominantly yield inclusion complexes with a 1:1 stoichiometric ratio<sup>2</sup>. However, two CD molecules are frequently bound to a single guest molecule to form a 2:1 CD-guest inclusion complex<sup>3-9</sup>. In some cases, a single CD molecule can accommodate two guest molecules to form a 1:2 CD-guest inclusion complex<sup>10-12</sup>.

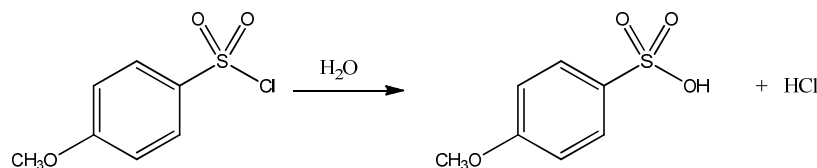
Surfactants are suitable model guests to perform detailed investigations on host:guest interactions with cyclodextrins because their structural properties can be easily modified. The length and number of alkyl chains can be varied along with the charge and size of the head group and such changes allow different complex structures and stoichiometries to be obtained. The interaction of  $\beta$ -CD with sodium alkylsulfonates<sup>13</sup>, sodium dodecyl sulfate (SDS) or tetradecyltrimethylammonium bromide (TTABr)<sup>14</sup> yields complexes with a 1:1 stoichiometric ratio. On changing from cetyl ( $C_{16}$ TACl) to octadecyltrimethylammonium chloride ( $C_{18}$ TACl), 1:1 and 2:1 complexes with  $\beta$ -CD can be formed<sup>15</sup>, respectively.

In comparison with other native cyclodextrins, the  $\gamma$ -derivative has a large cavity that can accommodate two molecules of appropriate size and shape<sup>16</sup>. When two guest molecules are located together within the CD cavity, one would expect them to interact with each other. This two-guest inclusion phenomenon was first reported in  $\gamma$ -CD-induced excimer fluorescence<sup>17</sup>. The possibility of the simultaneous formation of complexes with different stoichiometries must also be considered. For example,  $\gamma$ -CD

facilitated the formation of the ternary catalyst-substrate- $\gamma$ -CD complex in a 1:1:1 ratio and a redox reaction took place in this system<sup>17,18</sup>. Molecular interactions between an organic anion with  $\gamma$ -CD and several organic cations were investigated by means of absorption and fluorescence spectroscopy<sup>19</sup> and capillary electrophoresis<sup>20</sup>. The association between  $\gamma$ -CD and the organic anion yielded a negatively charged 1:1 inclusion complex with improved affinity for the inclusion of a second cationic guest. The results suggest that the formation of the ternary complex is favored with organic cations that bear long alkyl chains.

Our interest is currently focused on the use of cyclodextrins as molecular reactors, which are essentially miniature vessels for the assembly of reactants at the molecular level. The use of hosts for supramolecular catalysis will introduce new interactions that can be classified according to their nature: (i) Molecular interactions responsible for the formation of host:guest complexes may affect chemical reactivity by stabilizing intermediates and/or transition states. (ii) Molecular receptors can simply act as nanoscale reaction vessels by increasing local concentrations of reagents and thus the reaction rate. The aim of the work described here was to obtain evidence of the formation of three-component inclusion complexes and to study the role that the third component might play in promoting chemical reactivity. With this aim in mind, a kinetic study was carried out with the chemical probe 4-methoxybenzenesulfonyl chloride (MBSC, see Scheme 1), which is a molecule that has a suitable geometry and polarity for complex formation with  $\gamma$ -CD. A combination of kinetic and DOSY experiments provided evidence for the formation of different types of complexes in the presence of a surfactant<sup>21</sup>, C<sub>n</sub>TAB, as the third component. Different cyclodextrin binding mechanisms were observed for MBSC in the presence of the third component: the competitive mechanism with  $\beta$ -CD and the cooperative one with  $\gamma$ -CD lead to very different chemical reactivities.

Scheme 1



## EXPERIMENTAL SECTION

All chemicals used were of the highest commercially available purity and did not require further purification.  $\gamma$ -CD was supplied by Cyclolab. MBSC stock solutions were prepared in acetonitrile due to the instability of this material in water. The final acetonitrile concentration in the reaction medium was 1% (v/v).  $\gamma$ -CD/Surfactant systems were prepared by mixing appropriate volumes of stock aqueous  $\gamma$ -CD solutions and surfactant.

Kinetic runs were initiated by injecting an MBSC stock solution into the mixed system in a 1 cm cuvette. Stock solutions of MBSC were prepared in acetonitrile due to the low solubility of this compound in water. The final acetonitrile concentration in the reaction medium was 1% (v/v). Reaction kinetics were recorded by measuring absorbance due to the MBSC at 270 nm in a Cary 50 UV-Vis spectrophotometer (see Figure S-1, supporting information, for a reaction spectrum) with a cell holder thermostated at (25.0±0.1) °C. The MBSC concentration was  $1.0 \times 10^{-4}$  M in all cases. The absorbance-time data for all kinetic experiments were fitted by first-order integrated equations and the values of the pseudo-first-order rate constants,  $k_{obs}$ , were reproducible to within 3%. An example of the absorbance-time data fit to the first order rate equation for MBSC solvolysis is shown in Figure S-1 (see supporting information).

The electrical conductivity ( $\kappa$ ) was measured with a Crison conductivity meter calibrated using two KCl conductivity standard solutions supplied by Crison ([KCl] = 0.01 M,  $\kappa$  = 1413  $\mu$ S/cm at 25 °C and [KCl] = 0.1 M,  $\kappa$  = 12.88 mS/cm at 25 °C). The error in the accuracy of these measurements was  $\pm$  0.5%. During the measurements of electrical conductivity the temperature was regulated using a thermostat-cryostat with a precision of  $\pm$  0.1 °C. Solutions were prepared with doubly distilled water ( $\kappa$  = 0.1–0.50  $\mu$ S/cm). Electrical conductivity was used for cmc value determinations.

**NMR Experiments.** The stock solutions of  $\gamma$ -CD and C<sub>10</sub>TAB were prepared in D<sub>2</sub>O (99.9%) and the *para*-nitrophenyl acetate (NPA) stock solution was prepared in DMSO-*d*<sub>6</sub>. In order to study the complexation of NPA by  $\gamma$ -CD the ester concentration was kept constant, [NPA] = 1 mM, and the  $\gamma$ -CD concentration was varied. The C<sub>10</sub>TAB/ $\gamma$ -CD systems were prepared by mixing the appropriate volumes of stock solutions of  $\gamma$ -CD and C<sub>10</sub>TAB. In all cases the C<sub>10</sub>TAB concentration (12.5 mM) was kept constant, below the critical micellar concentration (cmc), and the  $\gamma$ -CD concentration was varied.

In the complexation process of NPA in the presence of the  $\gamma$ -CD/ $C_{10}$ TAB mixed system, the concentrations of NPA (1 mM) and  $\gamma$ -CD (27 mM) were kept constant and the concentration of  $C_{10}$ TAB was varied. Diffusion-Ordered NMR Spectroscopy (DOSY) was carried out at 25 °C on a Varian Inova 400 spectrometer. The DOSY spectra were acquired with the standard stimulated echo pulse using LED and bipolar gradient pulses<sup>22</sup>. Square-shaped pulsed gradients (G) of 2 ms duration were applied with the power level linearly incremented from 2 to 64.3 cm<sup>-1</sup> in 20 steps. To obtain reliable results for the diffusion coefficient, D, the diffusion time,  $\Delta$ , of the experiments was optimized for each sample to a value between 50 and 200 ms. The raw data were processed using the MestreC program.

Quantitative analysis of the intensity of a relevant echo peak in the diffusion spectrum provided the respective translational diffusion coefficient of the corresponding molecule. This was achieved by nonlinear fitting of the signal intensity to the Stejskal–Tanner equation<sup>23</sup>

$$I = I_0 \exp \left[ -D \gamma^2 G^2 \delta^2 \left( \Delta - \frac{\delta}{3} \right) \right] \quad (1)$$

where  $I$  is the measured signal intensity,  $I_0$  is the signal intensity at the lowest gradient pulse power,  $\gamma$  is the magnetogyric ratio of the observed nucleus, and the rest of the parameters are defined above. In all experiments, the intensity decay of the signals gave good fits to eq. 1, which shows that they represent a single self-diffusion coefficient. A typical plot of intensity decay vs  $\gamma^2 G^2 \delta^2 (\Delta - \delta/3)$  and the nonlinear fit to eq. 1 is shown in Figure 1.

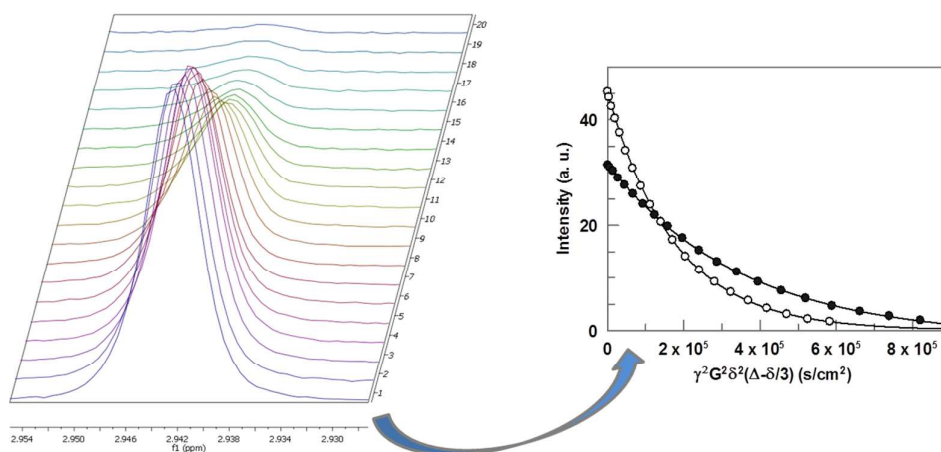


**Figure 1:** Representative echo decays for  $C_{10}$ TAB in the absence ( $\circ$ ) and in the presence of  $\gamma$ -CD (30 mM) ( $\bullet$ ). The data were fitted to an exponential function (solid lines).

## RESULTS AND DISCUSSION

The use of  $\gamma$ -CD as a reaction vessel in supramolecular catalysis requires a knowledge of the binding constants and stoichiometries of the species that act as guests. The large size of the  $\gamma$ -CD cavity in comparison with  $\alpha$ - or  $\beta$ -CD cavities means that the formation of 1:2 host:guest complexes should be considered. In order to evaluate this possibility and to gauge its influence on chemical reactivity we designed a system with two potential guests: a small organic molecule (NPA or MBSC) and a cationic surfactant. The preparation of different combinations of nitrophenyl acetate and the cationic surfactant would allow quantification of the simultaneous inclusion of two different guests by the  $\gamma$ -CD. Moreover, on using MBSC it is possible to assess the kinetic effect that the formation of complexes with different stoichiometries has on chemical reactivity.

The studies described in this section are presented in the following order: (i) the formation of 1:1 and 1:2 host:guest complexes in the individual systems formed by  $\gamma$ -CD and the cationic surfactant or  $\gamma$ -CD plus the small organic molecule (NPA) is discussed. (ii) The second step concerns an investigation into the formation of multiple complexes by the simultaneous addition of the cationic surfactant and NPA to a  $\gamma$ -CD solution. The formation of four different host:guest complexes, namely CD-NPA, CD-Surfactant, CD-Surfactant-Surfactant and CD-NPA-Surfactant, and their interconversion are discussed. (iii) The formation of different complexes will have important consequences for the chemical reactivity on using MBSC as a chemical probe.

**1. Homocomplexes (cationic and neutral) formed by  $\gamma$ -CD.** The ability of  $\gamma$ -CD to sequester two surfactant molecules to form 1:2 host:guest complexes is widely reported in the literature<sup>24</sup>. In order to quantify this process we analyzed the self-diffusion coefficients of the cationic surfactant C<sub>10</sub>TAB and the cyclodextrin. Formation of the inclusion complexes was studied by varying the concentration of  $\gamma$ -CD while keeping the surfactant concentration constant at a value well below its critical micelle concentration, cmc, in order to guarantee that only monomers were present in solution. The self-diffusion coefficients for C<sub>10</sub>TAB as a function of the [ $\gamma$ -CD] are represented in Figure 2. It should be noted that self-diffusion coefficients for  $\gamma$ -CD remain largely unaffected by the addition of surfactant, a finding in agreement with literature data for

$\beta$ -CD<sup>25</sup>. It can be observed that the self-diffusion coefficients for C<sub>10</sub>TAB decrease as the concentration of  $\gamma$ -CD increases, a trend that is due to the formation of an inclusion complex with  $\gamma$ -CD.

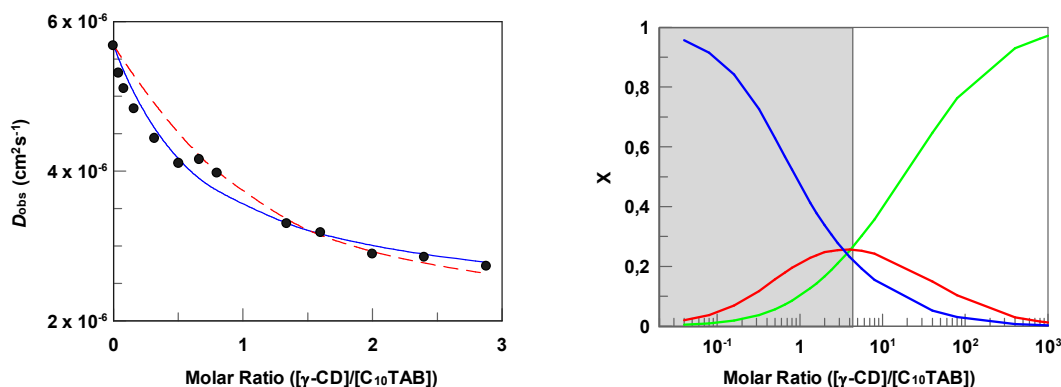


**Figure 2:** (Left) Self-diffusion coefficients for [C<sub>10</sub>TAB] = 12.5 mM on varying  $\gamma$ -CD concentrations. Lines show the fit to the model with a 1:1 complex (dashed line) and to the model with 1:1 and 1:2 host:guest complexes (solid line). (Right) Mole fraction (X) distribution of free C<sub>10</sub>TAB (blue line), 1:1 complex (green line) and 1:2 complex (red line). It should be noted that experimental conditions shown in the left-hand figure correspond to the dark region in the right-hand figure.

In order to carry out a quantitative analysis, the experimental data were fitted to a 1:1 complexation model (see section II in supporting information) and this yielded a binding constant  $K_{1:1}^{C_{10}TAB} = (225 \pm 25) \text{ M}^{-1}$ . As can be seen from Figure 2, this model (dashed line) mainly fails to reproduce the experimental behavior at low molar ratios where the percentage of 1:2 complex will be significant.

A model that takes into account the formation of 1:1 and 1:2 complexes allowed eq 2 to be derived and this reproduces the experimental data reasonably well (see section III in supporting information).

$$D_{obs}^{C_{10}TAB} = X_f^{C_{10}TAB} D_f^{C_{10}TAB} + X_{1:1}^{C_{10}TAB} D_{1:1}^{C_{10}TAB} + 2X_{1:2}^{C_{10}TAB} D_{1:2}^{C_{10}TAB} \quad (2)$$

As the concentration of  $\gamma$ -CD increases, the self-diffusion coefficients of the surfactant show a significant decrease, mainly due to the formation of a 1:2 inclusion complex with the  $\gamma$ -CD [Figure 2 (right, red line)]. A steady decrease in the self-diffusion coefficients is observed and this lower slope indicates an increase in the molar fraction of the 1:1 complex [Figure 2 (right, green line)]. In order to obtain the molar fractions

for the different species [i.e., free surfactant,  $X_f^{C_{10}TAB}$ , CD-Surfactant 1:1 complex,  $X_{1:1}^{C_{10}TAB}$ , and CD-(Surfactant)<sub>2</sub> 1:2 complex,  $X_{1:2}^{C_{10}TAB}$ ] it is necessary to know the values of the binding constants between  $\gamma$ -CD and C<sub>10</sub>TAB ( $K_{1:1}^{C_{10}TAB}$  and  $K_{1:2}^{C_{10}TAB}$ ). This equation was solved for different values of  $K_{1:1}^{C_{10}TAB}$  and  $K_{1:2}^{C_{10}TAB}$ , thus allowing the molar fractions of the different species at each  $\gamma$ -CD concentration to be obtained. The values of  $K_{1:1}^{C_{10}TAB}$  and  $K_{1:2}^{C_{10}TAB}$ , for which the best root-mean-square deviation ( $\chi^2$ ) values were obtained in the fitting of eq 2 to the experimental results were taken as optimal [see curve in Figure 2 (left)]. The use of this method gave the optimal values  $K_{1:1}^{C_{10}TAB} = (25 \pm 3) \text{ M}^{-1}$  and  $K_{1:2}^{C_{10}TAB} = (350 \pm 40) \text{ M}^{-1}$ . This fitting procedure also provided the values of the diffusion coefficients for free surfactant monomers,  $D_f^{C_{10}TAB} = (5.68 \pm 0.09) \times 10^{-6} \text{ cm}^2 \text{ s}^{-1}$ , 1:1 host:guest complex,  $D_{1:1}^{C_{10}TAB} = (2.0 \pm 0.1) \times 10^{-6} \text{ cm}^2 \text{ s}^{-1}$ , and 1:2 complex,  $D_{1:2}^{C_{10}TAB} = (1.50 \pm 0.1) \times 10^{-6} \text{ cm}^2 \text{ s}^{-1}$ . These results are consistent with an increase in the molecular weight due to the formation of the host:guest complexes. This experiment provided evidence for the formation of 1:1 and 1:2 inclusion complexes between  $\gamma$ -CD and C<sub>10</sub>TAB, in such a way that the formation of the 1:2 complex occurs in a cooperative mode. The formation of host:guest complexes by cyclodextrins is mainly driven by hydrophobic effects and van der Waals interactions. It has been reported that a large space remains in the  $\gamma$ -CD cavity of the 1:1 inclusion complex and this results in weak van de Waals interactions<sup>26</sup>. However, in the 1:2 complex, the area of the van de Waals contact between the host and the guest becomes significantly larger. Additionally, the cooperative effect observed in the formation of the 1:2 complex could be explained on the basis of the increase in the hydrophobic character of the  $\gamma$ -CD cavity upon formation of the 1:1 inclusion complex. The formation of inclusion complexes by cyclodextrins results in a release of water molecules from their cavity and this results in an increase in its hydrophobic character. Molecular dynamics simulations also support the formation of 1:1 and 1:2 inclusion complexes between the  $\gamma$ -CD and the anionic surfactant<sup>27</sup>.

The quantitative analysis of the inclusion behavior of small organic molecules will have important consequences on the modeling of their reactivity in the presence of cyclodextrins. The solvolysis of MBSC was used to model the behavior of the cyclodextrin cavity as a reaction vessel, but the low stability of this compound precludes the study of its inclusion behavior by NMR. NPA was used as an alternative

model compound as this molecule has a similar size, structure, and hydrophobicity. The influence of  $[\gamma\text{-CD}]$  on the self-diffusion coefficient of NPA is shown in Figure 3. The complexation process was investigated while keeping the NPA concentration constant (1 mM) and varying the  $\gamma\text{-CD}$  concentration. As can be observed, the self-diffusion coefficients of NPA decrease as a function of cyclodextrin concentration and this is due to the formation of an inclusion complex.

On using a similar procedure with  $\text{C}_{10}\text{TAB}$ , the data in Figure 3 can be fitted to the formation of a 1:1 host:guest complex. Under this assumption a value of  $K_{1:1}^{\text{NPA}} = (25 \pm 3) \text{ M}^{-1}$  was obtained for the binding constant and  $D_{1:1}^{\text{NPA}} = (2.0 \pm 0.1) \times 10^{-6} \text{ cm}^2\text{s}^{-1}$  for the self-diffusion coefficient of the host:guest complex. As the simultaneous formation of 1:1 and 1:2 complexes is observed with  $\text{C}_{10}\text{TAB}$ , this possibility was tested in the case of NPA. Under the assumption of a cooperative 1:2 complex different combinations of  $K_{1:1}^{\text{NPA}}$  and  $K_{1:2}^{\text{NPA}}$  values were tested where  $K_{1:2}^{\text{NPA}} > K_{1:1}^{\text{NPA}}$ . As an example, the situation with  $K_{1:1}^{\text{NPA}} = 25 \text{ M}^{-1}$  and  $K_{1:2}^{\text{NPA}} = 350 \text{ M}^{-1}$ , where the difference between the 1:1 and the 1:2 complexes is the same as with  $\text{C}_{10}\text{TAB}$ , is shown in Figure S-2 in the supporting information. Under this assumption the calculated self-diffusion coefficient is smaller than the experimental one, indicating that the fraction of bound NPA should be smaller than the predicted one. This discrepancy is a consequence of  $K_{1:2}^{\text{NPA}}$  being close to  $K_{1:1}^{\text{NPA}}$  due to the large volume of the NPA molecule in comparison with the alkyl chain of  $\text{C}_{10}\text{TAB}$ . Water molecules are released from the CD cavity upon formation of 1:1 complexes and this yields a more hydrophobic cavity, which in turn has a higher tendency to bind a second guest in a cooperative way. Meanwhile, formation of the 1:1 complex reduces the empty volume in the CD available to bind a second guest (1:2) and thus its binding constant is reduced. The balance between these two effects is responsible for the behavior observed. Accommodation of two NPA molecules inside the cavity is not as favorable as in the case of  $\text{C}_{10}\text{TAB}$  because of the larger volume occupied by the aromatic ring of the ester in comparison with the alkyl chain.

A simulation procedure similar to that described previously for  $\text{C}_{10}\text{TAB}$  (see section III in supporting information) allowed the optimal values (see Figure 3) for the NPA binding constants to be obtained:  $K_{1:1}^{\text{NPA}} = (20 \pm 3) \text{ M}^{-1}$  and  $K_{1:2}^{\text{NPA}} = (30 \pm 4) \text{ M}^{-1}$ .

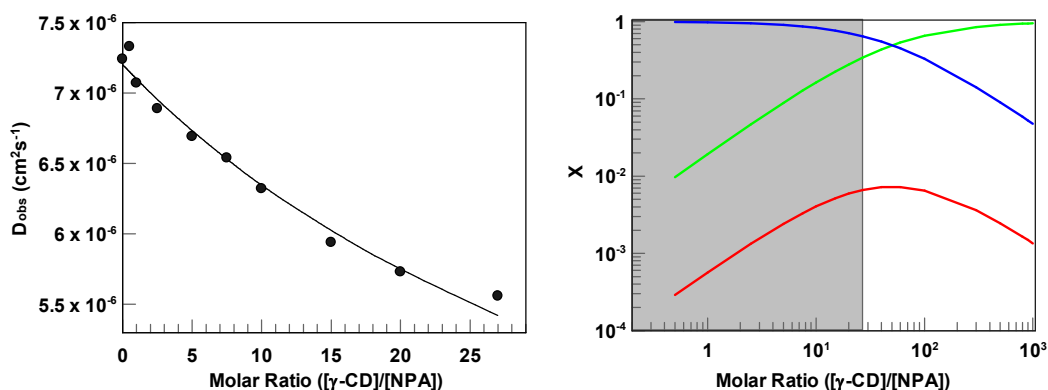


**Figure 3:** (Left) Self-diffusion coefficients for  $[NPA] = 1$  mM for varying  $\gamma$ -CD concentrations. The black line shows the fit to the model with 1:1 and 1:2 host:guest complexes. (Right) Respective mole fraction ( $X$ ) distribution of free NPA (blue line), 1:1 complex (green line) and 1:2 complex (red line). The experimental conditions shown in the left-hand figure correspond to the dark region in right-hand figure.

The species distribution shown in Figure 3 (right) can be calculated from the binding constants. As can be observed, the maximum fraction of 1:2 complex is less than 1% and it is almost negligible under the experimental conditions used in this study. As a consequence of this small percentage of 1:2 complex, the experimental results can be fitted to the exclusive formation of a 1:1 complex or the simultaneous inclusion of one and two guests.

**2. Heterocomplexes formed by  $\gamma$ -CD.** As both  $C_{10}TAB$  and NPA bind the  $\gamma$ -CD cavity it is possible to obtain mixed structures where 1:1:1 complexes are obtained in addition to the previously described 1:1 and 1:2 complexes. In order to study this type of heterocomplex the self-diffusion coefficients were determined by keeping the NPA (1 mM) and  $\gamma$ -CD (27 mM) concentrations constant and varying the cationic surfactant concentration. The observed self-diffusion coefficients for NPA and  $C_{10}TAB$  in the mixed system formed by  $\gamma$ -CD,  $C_{10}TAB$ , and NPA are shown in Figure 4.

From a qualitative point of view, the experimental data can be split into four different regions. For low  $C_{10}TAB$  concentrations,  $[C_{10}TAB] = 1 \times 10^{-3}$  M, the self-diffusion coefficient is much lower ( $D_{obs}^{C_{10}TAB} \sim 3.5 \times 10^{-6} \text{ cm}^2 \text{ s}^{-1}$ ) than the value obtained in pure water ( $D_f^{C_{10}TAB} = 5.68 \times 10^{-6} \text{ cm}^2 \text{ s}^{-1}$ ) due to its inclusion in the cyclodextrin cavity. Under these experimental conditions  $[\gamma\text{-CD}]/[C_{10}TAB] = 27$ , i.e., more than 90% of the  $C_{10}TAB$  is bound to the cyclodextrin in such a way that 55% of the surfactant forms 1:1 complexes and 35% is in the form of 1:2 host:guest complexes [see Figure 2

(right)]. On increasing the C<sub>10</sub>TAB concentration [regions I and II in Figure 4 (left)] the percentage of uncomplexed surfactant increases but its self-diffusion coefficients continue to decrease. This effect is a consequence of the formation of 1:2 complexes [from Figure 2 (right)] and one would expect a maximum fraction of 1:2 complexes at a molar ratio  $[\gamma\text{-CD}]/[\text{C}_{10}\text{TAB}] = 4$ , corresponding to a  $[\text{C}_{10}\text{TAB}] = 7 \times 10^{-3}$  M in Figure 4 (left). Region III in Figure 4 (left) corresponds to a situation where an excess of surfactant over cyclodextrin exists and the fraction of 1:2 complex predominates over the 1:1 complex. A small increase in the observed self-diffusion coefficient is expected because the diffusion is lower for the 1:2 than the 1:1 complex. A further increase in surfactant concentration [region IV in Figure 4 (left)] induces micellization and the surfactant self-diffusion coefficient drops very rapidly due to aggregation of this component.

The NPA self-diffusion coefficient as a function of C<sub>10</sub>TAB concentration in the presence of  $\gamma$ -CD is shown in Figure 4 (right). For a very low surfactant concentration,  $[\text{C}_{10}\text{TAB}] = 1 \times 10^{-3}$  M, the observed self-diffusion coefficient for NPA,  $D_{obs}^{NPA} \sim 5.0 \times 10^{-6} \text{ cm}^2 \text{ s}^{-1}$ , is smaller than its value in bulk water,  $D_f^{NPA} = 7.25 \times 10^{-6} \text{ cm}^2 \text{ s}^{-1}$ , but is compatible with the expected value for its complexation by  $\gamma$ -CD. An increase in the C<sub>10</sub>TAB concentration in the mixed system will decrease the cyclodextrin concentration available to bind the NPA because of the competitive binding of the surfactant. As a consequence of the competitive binding, one would expect the NPA self-diffusion coefficient to increase on increasing  $[\text{C}_{10}\text{TAB}]$ . The experimental results show the opposite behavior and this is a consequence of an additional complexation mode in the mixed system. The hydrophobicity of the cyclodextrin cavity increases upon surfactant inclusion to form 1:1 complexes because of the release of water. As a consequence, the ability to sequester NPA is much higher in the case of the  $\gamma$ -CD:surfactant host:guest complex than for pure cyclodextrin. This implies that a 1:1:1 heterocomplex in which both surfactant and NPA are simultaneously bound by  $\gamma$ -CD can be achieved. When  $[\text{C}_{10}\text{TAB}]$  is in the range from 7 to 50 mM [regions II and III in Figure 4 (right)] the percentage of cyclodextrin:surfactant with a 1:2 stoichiometry decreases from 25% to 18%, thus allowing the possibility of including NPA as a third component.

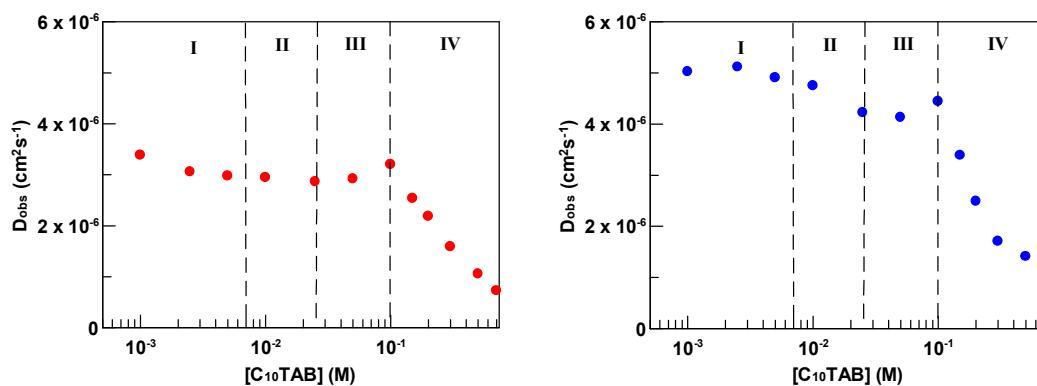


**Figure 4:** Observed self-diffusion coefficients for (●) C<sub>10</sub>TAB and (●) NPA for varying C<sub>10</sub>TAB concentrations and at [NPA] = 1 mM and [γ-CD] = 27 mM.

It can be seen from region III in Figure 4 (right) that the NPA self-diffusion coefficient increases at surfactant concentrations close to 100 mM. Under these conditions it can be estimated that almost 55% of the cyclodextrin is bound by the surfactant. This reduction in the amount of cyclodextrin available to bind the NPA results in a reduction in the fraction of bound NPA and, consequently, an increase in the self-diffusion coefficient is observed. A further increase in the surfactant concentration [region IV in Figure 4 (right)] induces self-aggregation to form micelles, with the consequent loss of NPA and a decrease in its diffusion coefficient. It should be noted that the self-diffusion coefficient for NPA is higher than that for C<sub>10</sub>TAB in I, II, and III in Figure 4 because of the different size and molecular weight. However, these diffusion coefficients are almost equal in the presence of high surfactant concentrations (e.g., high concentrations in region IV of Figure 4). This effect occurs because most of the surfactant is aggregated in the micelles (where NPA is dissolved) and the micelle and the dissolved NPA both have the same diffusive behavior.

**3. Influence of simultaneous complexation on chemical reactivity.** The aim of this work was to quantitatively evaluate the γ-CD cavity as a reaction medium and to assess the influence of multiple complexation. To this end, the solvolysis of 4-methoxybenzenesulfonyl chloride, MBSC, was used as a chemical probe. This reaction is suitable for this purpose because the size of MBSC allows multiple complexation and it is a solvolytic process that is affected by the properties of the medium in such a way that the reaction rate decreases by a factor close to 10<sup>2</sup> on changing from water to 90% ethanol:water<sup>28</sup>. The observed solvolytic rate constant,  $k_{obs}$ , allowed the

complexation process of MBSC by  $\gamma$ -CD to be studied. The observed rate constant was experimentally obtained in a series of experiments in which the MBSC concentration (0.1 mM) was kept constant and the  $\gamma$ -CD concentration was varied from  $[\gamma\text{-CD}] = 2$  mM to 100 mM. As can be seen from Figure 5, the observed rate constant decreased on increasing the cyclodextrin concentration. This experimental behavior is due to the incorporation of MBSC within the cyclodextrin cavity, where the solvolytic reaction is much slower than in bulk water as a consequence of the lower polarity of this space.

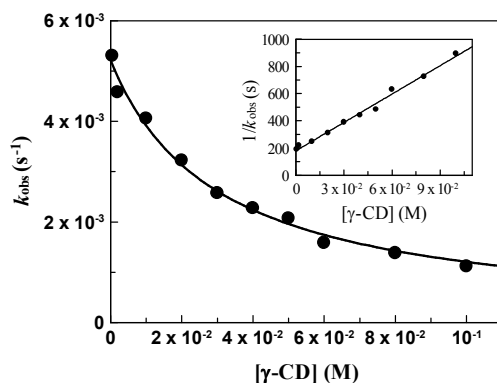
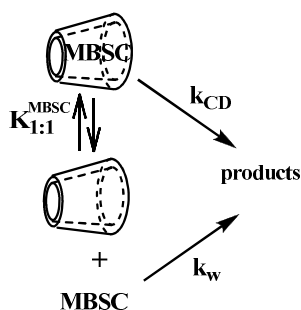


**Figure 5:** Influence of  $\gamma$ -CD concentration on  $k_{\text{obs}}$  for the hydrolysis of MBSC at 25.0 °C. Curve representation fits the experimental data to equation 3.

In order to analyze the results in Figure 5 quantitatively it is necessary to propose a complexation scheme between MBSC and  $\gamma$ -CD. It will be shown that not only the size but also the binding constants of NPA and MBSC are similar. Based on this information one would expect the possibility of binding one or two MBSC molecules within the cyclodextrin cavity. However, a close examination of the species distribution shown in Figure 3 (right) allowed us to discard the minimum percentage of inclusion complex with a 1:2 stoichiometry. Under the kinetic experimental conditions the ratio  $[\gamma\text{-CD}]/[\text{MBSC}]$  ranges from 20 to  $10^3$ , i.e., the percentage of 1:2 complex is less than 0.5%. Given this information the kinetic behavior can be explained by Scheme 2, where the solvolytic reaction takes place simultaneously in two well-differentiated environments: water ( $k_w$ ) and the  $\gamma$ -CD cavity ( $k_{\text{CD}}$ ).

Scheme 2



The following rate equation can be derived from Scheme 2, where  $K_{1:1}^{MBSC}$  is the binding equilibrium constant of MBSC to the  $\gamma$ -CD,  $k_{CD}$  is the rate constant for the reaction in the cavity of  $\gamma$ -CD, and  $k_w$  is the rate constant for solvolysis in the aqueous medium.

$$k_{obs} = \frac{k_w + K_{1:1}^{MBSC} k_{CD} [CD]}{1 + K_{1:1}^{MBSC} [CD]} \quad (3)$$

On considering that the solvolytic rate constant is much larger in water than in the cyclodextrin cavity, and because the binding equilibrium constant is small, the inequality ( $k_w \gg K_{1:1}^{MBSC} k_{CD} [CD]$ ) can be considered. On the basis of this assumption equation 3 can be simplified to equation 4, which can be rewritten as a function of its inverse. This latter equation predicts a linear dependence between  $1/k_{obs}$  and  $[CD]$  (Figure 5, inset).

$$k_{obs} = \frac{k_w}{1 + K_{1:1}^{MBSC} [CD]} \quad \text{or} \quad \frac{1}{k_{obs}} = \frac{1}{k_w} + \frac{K_{1:1}^{MBSC}}{k_w} [CD] \quad (4)$$

Equation 4 provides a good fit to the experimental data (Figure 5, inset), from which the parameters  $k_w = (5.7 \pm 0.1) \times 10^{-3} \text{ s}^{-1}$  and  $K_{1:1}^{MBSC} = (38 \pm 2) \text{ M}^{-1}$  were obtained, with the latter value similar to that observed for NPA ( $K_{1:1}^{NPA} = 20 \text{ M}^{-1}$ ).

Prior to the reactivity study in the three-component system ( $\gamma$ -CD/surfactant/MBSC) it was necessary to analyze the influence of surfactant concentration on the solvolytic rate constant. The observed rate constant,  $k_{obs}$ , is unaffected by the addition of small amounts of surfactant up to the critical micelle concentration, as shown in Section V in the supporting information. A further increase

in surfactant concentration results in both micelle formation and the incorporation of MBSC in the micellar core. As a consequence,  $k_{obs}$  decreases on increasing the surfactant concentration. This kinetic behavior is well documented in the literature<sup>29</sup> and analysis of the data provides both the binding constant of MBSC to the micellar core,  $K_m^{MBSC}$ , and the solvolytic rate constant inside the micelle,  $k_m$ . As shown in Section V of the supporting information, the MBSC binding constant increases on increasing the alkyl chain length of the surfactant (C<sub>8</sub>TAB; C<sub>10</sub>TAB; C<sub>14</sub>TAB and C<sub>18</sub>TACl) due to the corresponding increase in hydrophobic character.

Solvolysis of MBSC in a three component system ( $\gamma$ -CD/surfactant/MBSC) was studied by keeping the MBSC and  $\gamma$ -CD concentrations constant at 0.1 and 20 mM, respectively, and varying the [C<sub>10</sub>TAB]. As an example, the results obtained on using C<sub>10</sub>TAB in the presence of  $\gamma$ -CD are shown in Figure 6 (see Figure S-7 in the supporting information for other surfactants). The complex kinetic behavior observed is qualitatively the same regardless of the alkyl chain length of the surfactant.

A kinetic model to explain reactivity in the cyclodextrin/surfactant mixed system has recently been developed in our group<sup>30</sup>. The kinetic model is a combination of the traditional pseudophase model, which includes ion exchange, and a competitive binding model for the CD-catalyzed reaction. Some characteristics of mixed CD-surfactant systems can be highlighted: (i) a complexation equilibrium between the surfactant and the cyclodextrin can be established. As the surfactant concentration increases, the concentration of uncomplexed surfactant monomers in equilibrium with the CD is sufficient for the micellization process to begin. (ii) The critical micelle concentration has been found to shift to higher values in the presence of CD. (iii) Once the micellization has started, interactions between CD and the micellar system will not be established. (iv) At the micellization point an appreciable concentration of uncomplexed CD must exist,  $[CD]_f$ .

It can be seen from the solid line in Figure 6 that the competitive binding model (see section VIII in supporting information) fails to explain the kinetic behavior. The competitive binding model does not take into consideration the formation of heterocomplexes, i.e., it only considers the formation of 1:1 and 1:2 homocomplexes with C<sub>10</sub>TAB and a competitive binding of MBSC displacing C<sub>10</sub>TAB to the bulk aqueous media. The competitive binding model predicts that  $k_{obs}$  values increase on increasing [C<sub>10</sub>TAB] due to its competitive binding and release of MBSC to bulk water,

where its solvolytic rate constant is much higher than that in the cyclodextrin cavity. The observed rate constant increases up to a maximum value where the concentration of free surfactant monomers is sufficient for micellization to occur. A further increase in  $C_{10}TAB$  concentration increases the number of micelles available for MBSC solubilization in such a way that the kinetic behavior parallels that observed in the presence of pure micellar aggregates. It can be observed that there is a large discrepancy between the calculated and the observed rate constants, with the calculated values being much higher than the experimentally obtained ones. As discussed below, this discrepancy is mainly due to the omission of the MBSC:CD: $C_{10}TAB$  1:1:1 cooperative complex in the reaction scheme.

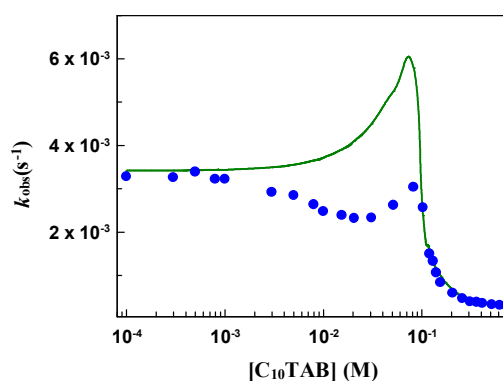


**Figure 6:** Influence of the surfactant concentration on  $k_{obs}$  for the hydrolysis of MBSC at 25.0 °C in the presence of  $\gamma$ -CD and  $C_{10}TAB$ . [ $\gamma$ -CD] =  $2 \times 10^{-2}$  M; [MBSC] =  $1 \times 10^{-4}$  M. The solid line signifies calculated values corresponding to a competitive binding by the cyclodextrin (see text).

On considering the results obtained previously from DOSY experiments it is easy to understand the experimental behavior represented in Figures 6 and 7 from a qualitative point of view. Four different regions can be considered to explain the influence of  $[C_{10}TAB]$  on  $k_{obs}$ : (i) For very small  $[C_{10}TAB]$  (charts A and B in Figure 7) there is a large excess of  $\gamma$ -CD and the observed kinetic behavior is due to the inclusion of MBSC and  $C_{10}TAB$  in the cyclodextrin cavity. The large excess of  $\gamma$ -CD in comparison with available guests means that the magnitude of  $k_{obs}$  is unaffected. (ii) For  $[C_{10}TAB]$  ranging from (1–20) mM the observed rate constant decreases on increasing the surfactant concentration. The formation of a 1:1:1 complex takes place in this region (chart C in Figure 7), thus increasing the total amount of MBSC incorporated in the cyclodextrin cavity and, consequently, decreasing its solvolytic reaction rate. (iii) An

increase of  $k_{obs}$  with the surfactant concentration is observed in the region of  $[C_{10}TAB] = (20-90)$  mM. In this concentration range the formation of 1:2 host:guest complexes between  $\gamma$ -CD and  $C_{10}TAB$  is observed along with the concomitant release of MBSC from the 1:1:1 complex to bulk water. (iv) A further increase in the surfactant concentration,  $[C_{10}TAB] > 100$  mM, induces self-aggregation to form micelles along with a consequent decrease in  $k_{obs}$  due to MBSC as a consequence of its incorporation within the hydrophobic micellar core.

Once the micelles are formed, an inhibitory effect is observed because MBSC is incorporated into the micelles. Therefore, the minimal surfactant concentration necessary to observe an appreciable change in the maximum of  $k_{obs}$  is attributed to the micellization point. It is important to mention that independent experiments confirmed that the maximum in Figure 7 (observed for  $[C_{10}TAB]$  close to 100 mM) corresponds to surfactant micellization under the reaction conditions. Under these experimental conditions the critical micelle concentration was obtained from conductivity experiments (see Figures S-5 and S-6 in supporting information), which gave a value of  $cmc = 100$  mM.

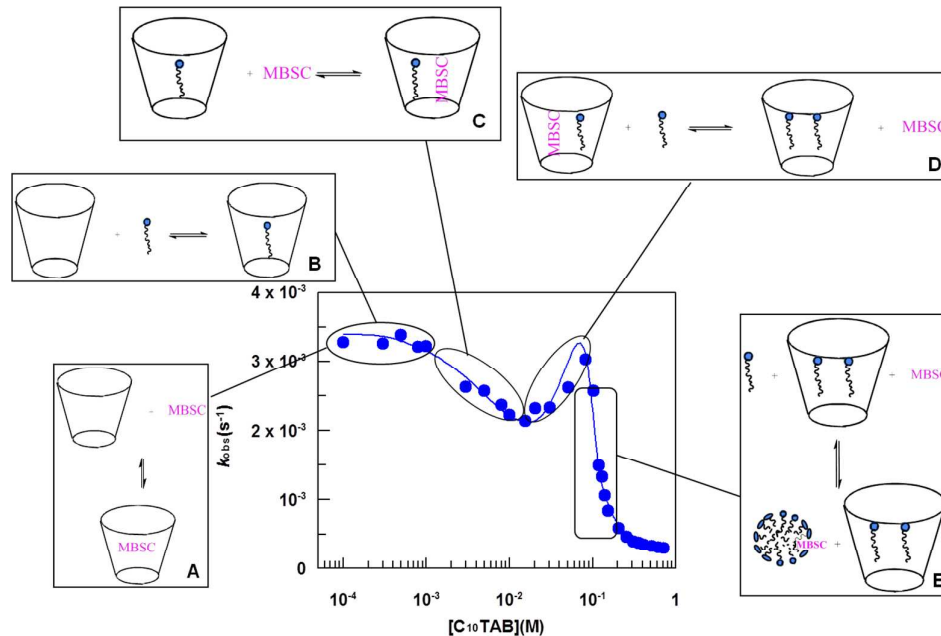
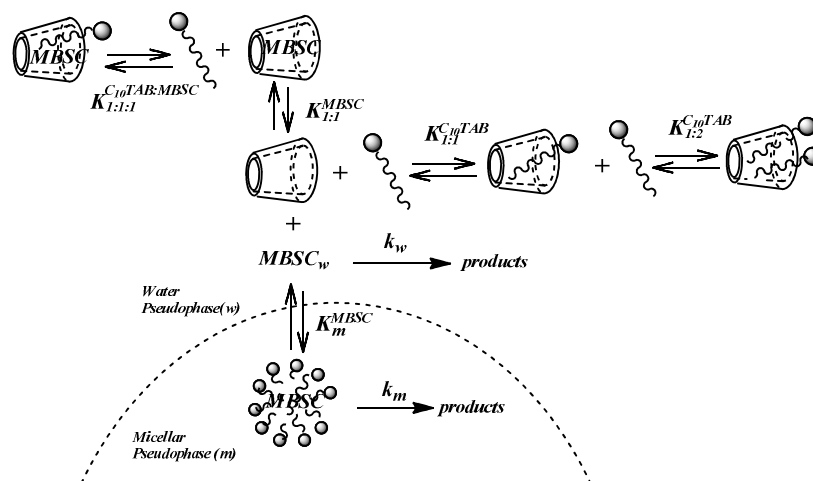


**Figure 7:** Influence of the surfactant concentration on  $k_{obs}$  for the hydrolysis of MBSC at 25.0 °C in the presence of  $\gamma$ -CD and  $C_{10}TAB$ .  $[\gamma\text{-CD}] = 2 \times 10^{-2}$  M;  $[\text{MBSC}] = 1 \times 10^{-4}$  M. The solid line corresponds to the fit of equation 5 to the experimental data.

The maximum observed in the plot of  $k_{obs}$  vs. surfactant concentration is due to surfactant micellization. As can be observed in Figure S-7 in the supporting information, the amount of surfactant needed for micellization in the presence of  $[\gamma\text{-CD}] = 20$  mM increases in the order  $\text{C}_{18}\text{TACl}$  (ca. 15 mM),  $\text{C}_{14}\text{TAB}$  (ca. 22 mM);  $\text{C}_{10}\text{TAB}$  (ca. 100 mM), and  $\text{C}_8\text{TAB}$  (ca. 250 mM). These values follow the trend in the critical micelle concentrations in the absence of cyclodextrin:  $\text{C}_{18}\text{TACl}$  (0.22 mM),  $\text{C}_{14}\text{TAB}$  (3.5 mM),  $\text{C}_{10}\text{TAB}$  (60 mM), and  $\text{C}_8\text{TAB}$  (200 mM). The addition of cyclodextrin to a surfactant solution increases the critical micelle concentration due to the inclusion of surfactant in the CD cavity. This effect on the critical micelle concentration depends on the balance between cyclodextrin complexation and surfactant self-aggregation in such a way that a significant fraction of uncomplexed cyclodextrin coexists with the micellar system.

Previous studies on mixed systems formed by  $\beta\text{-CD}$  and surfactants have shown a competitive complexation scheme. In these studies<sup>31</sup> the competitive formation of an inclusion complex between the surfactant and  $\beta\text{-CD}$  leads to the release of MBSC to bulk water and this gives rise to an increase in the observed rate constant. On the basis of the information depicted in Figure 6, this possibility can be ruled out in the case of  $\gamma\text{-CD}$  because the large size of the cavity allows multiple complexation. The kinetic model should be broadened in the present case in order to take into account the possibility of multiple complexation in a cooperative way. The actual kinetic model is depicted in Scheme 3, where the absence of interactions between micelles and  $\gamma\text{-CD}$  as well as the existence of two simultaneous reaction paths are considered: the reaction of the free substrate in the aqueous medium,  $k_w$ , and the reaction of the substrate associated with the micelle,  $k_m$ . As shown previously, the reaction of the substrate bound to the  $\gamma\text{-CD}$  can be neglected because of the low polarity of its cavity. The release of water from the cyclodextrin cavity in multiple complexation (1:1:1) is greater than for binary complexes, thus resulting in a cavity with a lower polarity. The solvolytic rate constant in the ternary 1:1:1 complex is expected to be much lower than in the 1:1 complex and, as a consequence, this can be neglected.

Scheme 3



This mechanistic scheme allowed us to derive the following expression for the observed rate constant:

$$k_{obs} = \frac{k_w + k_m K_m^{MBSC} [D_n]}{1 + K_m^{MBSC} [D_n] + K_{1:1}^{MBSC} [CD]_f + K_{1:1}^{C_{10}TAB} [C_{10}TAB] [CD]_f} \quad (5)$$

To solve the above equation it is necessary to know the concentration of micellized surfactant in the mixed system,  $[D_n]$ , and this is obtained as the total surfactant concentration minus the critical micelle concentration of the mixed system. The critical micelle concentration is assumed to be the surfactant concentration corresponding to the maximum value of  $k_{obs}$  in Figure 7 (close to 100 mM). It is important to note that this assumption was confirmed by conductimetric determination of the cmc (see Figures S-5 and S-6 in the supporting information). Moreover, it is necessary to know the concentration of uncomplexed cyclodextrin,  $[CD]_f$ , for each surfactant concentration. This value can be obtained from binding constants taking into account simultaneous substrate complexation by CD,  $K_{1:1}^{MBSC}$ , surfactant complexation with a 1:1,  $K_{1:1}^{C_{10}TAB}$ , and 1:2 stoichiometry,  $K_{1:2}^{C_{10}TAB}$ , as well as ternary complexes with the simultaneous inclusion of MBSC and surfactant,  $K_{1:1:1}^{C_{10}TAB:MBSC}$ .

$$K_{1:1}^{MBSC} = \frac{[CD:MBSC]}{[MBSC]_w [CD]_f} \quad K_{1:1}^{C_{10}TAB} = \frac{[CD:C_{10}TAB]}{[CD]_f [C_{10}TAB]} \quad (6)$$

$$K_{1:2}^{C_{10}TAB} = \frac{[CD:(C_{10}TAB)_2]}{[CD:C_{10}TAB][C_{10}TAB]} \quad K_{1:1:1}^{C_{10}TAB:MBSC} = \frac{[MBSC:CD:C_{10}TAB]}{[MBSC][CD:C_{10}TAB]}$$

The mass balances for the total concentrations of  $\gamma$ -CD, surfactant, and substrate for surfactant concentrations below the critical micelle concentration are:

$$[CD]_T = [CD]_f + [CD:MBSC] + [CD:C_{10}TAB] + [CD:(C_{10}TAB)_2] + [MBSC:CD:C_{10}TAB] \quad (7)$$

$$[S]_T = [S]_f + [CD:C_{10}TAB] + 2[CD:(C_{10}TAB)_2] + [MBSC:CD:C_{10}TAB] \quad (8)$$

$$[MBSC]_T = [MBSC]_f + [CD:MBSC] + [MBSC:CD:C_{10}TAB] \quad (9)$$

In order to obtain  $[CD]_f$  the values of  $K_{1:1}^{MBSC}$ ,  $K_{1:1}^{C_{10}TAB}$ ,  $K_{1:2}^{C_{10}TAB}$ , and  $K_{1:1:1}^{C_{10}TAB:MBSC}$  are required. The values of  $K_{1:1}^{C_{10}TAB}$  and  $K_{1:2}^{C_{10}TAB}$  were previously determined by DOSY experiments. The binding constant for MBSC to  $\gamma$ -CD,  $K_{1:1}^{MBSC}$  was previously obtained from kinetic experiments carried out in the absence of  $C_{10}TAB$ . In order to obtain the value of  $K_{1:1:1}^{C_{10}TAB:MBSC}$ , the above equations were solved for different values of  $K_{1:1:1}^{C_{10}TAB:MBSC}$  and this provided the concentration of uncomplexed  $\gamma$ -CD for each surfactant concentration. The  $[CD]_f$  values and the  $[D_n]$  values can be used to fit the experimental  $k_{obs}$  values to equation 5 (solid curve in Figure 7). The value of  $K_{1:1:1}^{C_{10}TAB:MBSC}$ , for which the best root-mean-square deviation ( $\chi^2$ ) values were obtained in the fitting of eq. 5 to the experimental results, was taken as optimal. From this method the optimal value  $K_{1:1:1}^{C_{10}TAB:MBSC} = 585 \text{ M}^{-1}$  was obtained. Moreover, fitting of the experimental results to eq. 5 by a nonlinear regression method provided the values for the distribution constant of MBSC between the water and the micellar pseudophase,  $K_m = 90 \text{ M}^{-1}$ , the rate constant in the micellar pseudophase,  $k_m = 1.8 \times 10^{-4} \text{ s}^{-1}$ , and the rate constant in water,  $k_w = 5.7 \times 10^{-3} \text{ s}^{-1}$ . It should be mentioned that the value for the ternary complex,  $K_{1:1:1}^{C_{10}TAB:MBSC} = 585 \text{ M}^{-1}$ , is much higher than that obtained when both guests are the same. In the case of the  $C_{10}TAB$  surfactant a value of  $K_{1:2}^{C_{10}TAB} = 350 \text{ M}^{-1}$  was obtained and for NPA, a guest with similar structure to MBSC, a value of  $K_{1:2}^{NPA} = 30 \text{ M}^{-1}$  was obtained. It is thought that these results are a consequence of the perfect fit in the  $\gamma$ -CD cavity of the alkyl chain of the surfactant and the MBSC.

The formation of a ternary complex is of major importance in the reaction pathway. Values of  $k_{obs}$  are very useful to obtain  $[CD]_f$  in cases where a competitive complexation mechanism operates<sup>13-15</sup>. In this situation the calibration curve can be obtained by regrouping equation 4 and using previously obtained values for  $K_{1:1}^{MBSC}$  and  $k_w$ . According to this procedure, and on using the  $k_{obs}$  values at the maximum,  $k_{obs} = 3.2 \times 10^{-3} \text{ s}^{-1}$ , a value of  $[CD]_f = 11.5 \text{ mM}$  can be calculated and this indicates that almost 57% of the cyclodextrin is uncomplexed in equilibrium with the micellar systems formed by C<sub>10</sub>TAB. This value is much higher than that obtained from equilibrium constants,  $[CD]_f = 0.54 \text{ mM}$ , which correspond to 2.7% uncomplexed cyclodextrin. The main reason for this discrepancy is that the calibration procedure does not take into account the formation of ternary 1:1:1 complexes.

Equations 6–9 can be used to calculate the concentration distribution of the different species that are present in the mixed system (see Figure 8) before the micellization process begins ( $[C_{10}TAB] = 0.1 \text{ M}$ ). Firstly, it should be mentioned that there is a non-zero concentration of uncomplexed  $\gamma$ -CD. This result is consistent with previous studies in our laboratory, in which it was found that saturation of the cyclodextrin complexation ability is not necessary prior to micellization. Instead, cyclodextrin complexation and surfactant self-assembly are processes that take place simultaneously and the balance between them should be responsible for the existence of  $[CD]_f$  in equilibrium with the micellar system. The percentage of uncomplexed cyclodextrin<sup>15</sup> increases both on decreasing and increasing the surfactant hydrophobicity, with a minimum value found for alkyl chains close to 10 carbon atoms. On decreasing the hydrophobicity the predominant effect is the low tendency to complex formation by the cyclodextrin cavity. Surfactants with very high hydrophobicity bind strongly to cyclodextrins but their ability to self-assemble also increases to the extent that micellization predominates over cyclodextrin complexation.

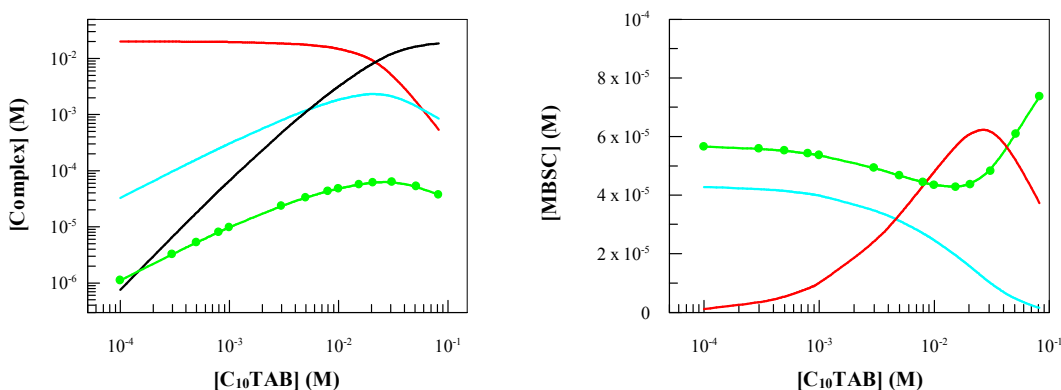


**Figure 8:** (Left) Concentration distribution of  $[CD]_f$  (red line); CD: $C_{10}TAB$  complex (blue line); CD:( $C_{10}TAB$ )<sub>2</sub> complex (black line) and MBSC:CD: $C_{10}TAB$  ternary complex (green line) as a function of  $[C_{10}TAB]$  in the presence of  $[\gamma\text{-CD}] = 2 \times 10^{-2}$  M. (Right) Concentration distribution of uncomplexed MBSC (green line); CD:MBSC complex (blue line) and MBSC:CD: $C_{10}TAB$  ternary complex (red line) as a function of  $[C_{10}TAB]$  in the presence of  $[\gamma\text{-CD}] = 2 \times 10^{-2}$  M.

It can be seen from Figure 8 (left) that the CD: $C_{10}TAB$  1:1 complex predominates over the CD:( $C_{10}TAB$ )<sub>2</sub> 1:2 complex for regions with a large excess of cyclodextrin over surfactant. When the ratio  $[CD]/[C_{10}TAB]$  approaches unity or increases beyond this point, the higher stoichiometric complex predominates. It should be noted that the concentration of the 1:2 complex reaches a limiting value on increasing the surfactant concentration because almost all of the cyclodextrin is complexed. Under these conditions a further increase in  $C_{10}TAB$  cannot yield more complex due to the absence of available cyclodextrin. More relevant for the present study is the fact that the evolution of the 1:1:1 complex increases with  $C_{10}TAB$  concentration up to a maximum value, after which it decreases in the presence of a large excess of surfactant when the 1:2 complex predominates. The concentration of this complex is much lower than that of the CD: $C_{10}TAB$  1:1 and CD:( $C_{10}TAB$ )<sub>2</sub> complexes as a result of the large excess of  $\gamma\text{-CD}$  (20 mM) in comparison with MBSC (0.1 mM).

The situation depicted in Figure 8 (right) has significant implications on chemical reactivity results because different states of MBSC are shown. From a kinetic point of view, it should be mentioned that only the uncomplexed MBSC contributes to the solvolytic rate constant. In fact, it can be observed that the kinetic profile shown in Figure 7 parallels the uncomplexed MBSC concentration profile shown in Figure 8. It should be noted that almost 60% of uncomplexed MBSC is present at very low  $C_{10}TAB$  concentration. On increasing the surfactant concentration the percentage of CD:MBSC 1:1 complex decreases, as one would expect from a competitive binding situation, but

the molar fraction of MBSC:CD:C<sub>10</sub>TAB increases due to cooperative binding. As a consequence of the cooperative binding, the 1:1:1 complex is the predominant species until [C<sub>10</sub>TAB] is equal to 30 mM. A further increase in surfactant concentration leads to an increase in the percentage of the CD:(C<sub>10</sub>TAB)<sub>2</sub> 1:2 complex and a decrease in the concentration of the 1:1:1 ternary one, with a consequent increase in the uncomplexed MBSC concentration. This increase in the concentration of uncomplexed MBSC is the reason why  $k_{obs}$  increases prior to surfactant micellization in Figure 7. We have shown previously that the calibration method failed in calculating the fraction of uncomplexed cyclodextrin in equilibrium with the micellar system. This failure is due to an inherent limitation in the calibration procedure because both the 1:1 CD:MBSC and 1:1:1 MBSC:CD:C<sub>10</sub>TAB are kinetically silent from the point of view of solvolytic reactivity. As a consequence, the value of the observed rate constant at the micellization point is attributed to the balance between free MBSC and 1:1 complex but the existence of the ternary 1:1:1 complex is ignored.

## CONCLUSIONS

The results obtained from kinetic and DOSY experiments allowed us to conclude that  $\gamma$ -CD molecules can form different types of complexes (1:1, 1:2 and 1:1:1) with two guests operating simultaneously. A cooperative effect is observed in the formation of the ternary heterocomplexes (1:1:1) as in the case of the surfactant complexation. This behavior is in contrast to that observed with  $\beta$ -CD, for which competitive formation of the  $\beta$ -CD:surfactant inclusion complexes is observed. In the case of  $\beta$ -CD, the formation of these inclusion complexes displaces the MBSC to the aqueous medium. However, in the case of  $\gamma$ -CD a binary inclusion complex  $\gamma$ -CD:MBSC (1:1 complex) is observed first and a further increase in surfactant concentration induces the formation of a hetero inclusion complex formed by  $\gamma$ -CD:surfactant:MBSC (1:1:1 complex). Finally, a subsequent increase in surfactant concentration leads to the formation of a  $\gamma$ -CD:(surfactant)<sub>2</sub> (1:2 complex) in a competitive way, which displaces the MBSC to the aqueous medium. As a consequence of this multiple complexation the chemical reactivity shows very complex behavior.

## ACKNOWLEDGMENTS

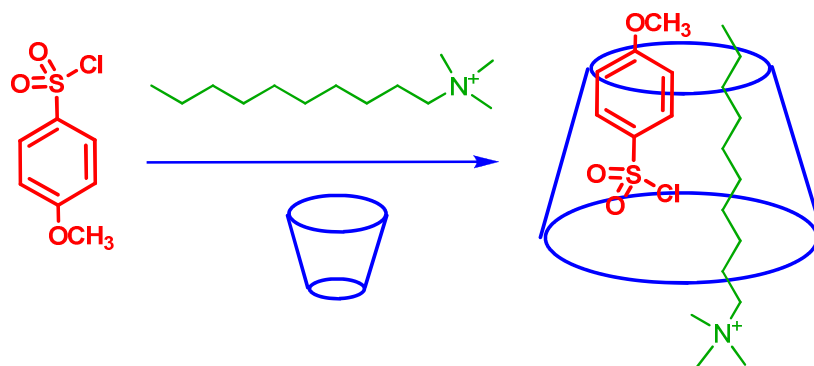
Financial support from the Ministerio de Economía y Competitividad (Project CTQ2011-22436) and Xunta de Galicia (PGIDIT10-PXIB209113PR and 2007/085). J. F.-R. thanks the Ministerio de Economía y Competitividad for an FPI fellowship (BES-2012-054593). M.P. acknowledges the Fundação para a Ciência e Tecnologia (FCT, Portugal) and POPH/FSE for a Ph.D. grant (Grant SFRH/BD/60911/2009). N.B. acknowledges funding for a postdoctoral grant (SFRH/BPD/84805/2012).

**BIBLIOGRAPHY**

- [1] W. Saenger, *Angew. Chem. Int. Ed.*, 1980, **19**, 344–362.
- [2] M. L. Bender, M. Komiyama, *Cyclodextrin Chemistry*, Springer-Verlag, New York, 1978.
- [3] H. R. Park, B. Mayer, P. Wolschann, G. Kohler, *J. Phys. Chem.*, 1994, **98**, 6158–6166.
- [4] E. K. Fraiji, T. R. Cregan, T. C. Werner, *Appl. Spectrosc.*, 1994, **48**, 79–84.
- [5] J. M. Ribó, J.-A. Farrera, M. L. Valero, A. Virgili, *Tetrahedron*, 1995, **51**, 3705–3712.
- [6] G. M. Escandar, *Analyst*, 1999, **124**, 587–591.
- [7] S. Hamai, *J. Phys. Chem.*, 1995, **99**, 12109–12114.
- [8] S. Hamai, *J. Phys. Chem. B*, 1997, **101**, 1707–1712.
- [9] S. Hamai, T. Kudou, *J. Photochem. Photobiol. A: Chem.*, 1998, **113**, 135–140.
- [10] T. Tamaki, T. Kokubu, *J. Inclusion Phenom.*, 1984, **2**, 815–822.
- [11] R. J. Clarke, J. H. Coates, S. F. Lincoln, *J. Chem. Soc., Faraday Trans. I*, 1986, **82**, 2333–2343.
- [12] (a) A. Piñeiro, X. Banquy, S. Pérez-Casas, E. Tovar, A. García, A. Villa, A. Amigo, A. E. Mark, M. Costas, *J. Phys. Chem. B*, 2007, **111**, 4383–4392. (b) S. Hamai, *Bull. Chem. Soc. Jpn.*, 2007, **80**, 1527–1533. (c) C. Yang, G. Fukuhara, A. Nakamura, Y. Origane, T. Mori, T. Wada, Y. Inoue, *J. Incl. Phenom. Macrocycl. Chem.*, 2007, **57**, 433–437. (d) R. A. Agaria, E. Roberts, I. M. Warner, *J. Phys. Chem.*, 1995, **99**, 10056–10060. (e) J. Andreaus, J. Draxler, R. Marr, A. Hermetter, *J. Coll. Interface Sci.*, 1997, **193**, 8–16.
- [13] M. Cepeda, R. Daviña, L. García-Río, M. Parajó, *Chem. Phys. Lett.*, 2010, **499**, 70–74.
- [14] L. García-Río, M. Méndez, M. R. Paleo, F. J. Sardina, *J. Phys. Chem. B*, 2007, **111**, 12756–12764.
- [15] M. Cepeda, R. Daviña, L. García-Río, M. Parajó, P. Rodríguez-Dafonte, M. Pessêgo, *Org. Biomol. Chem.*, 2013, **11**, 1093–1102.
- [16] M. V. Rekharsky, Y. Inoue, *Chem. Rev.*, 1998, **98**, 1875–1918.
- [17] A. Ueno, K. Takahashi, T. Osa, *J. Chem. Soc., Chem. Commun.*, 1980, 921–922.
- [18] K. Takahashi, *Studies on the control of various aqueous reactions by host-guest complexation of cyclodextrins*, Pharmaceutical Institute Tohoku University, 1986.
- [19] S. Hamai, *Bull. Chem. Soc. Jpn.*, 2007, **80**, 1527–1533.

- [20] S. Hamai, Y. Sasaki, T. Hori, A. Takahashi, *J. Inclusion Phenom. Macrocyclic Chem.*, 2006, **54**, 67–76.
- [21] The nomenclature C<sub>8</sub>TAB, C<sub>10</sub>TAB, C<sub>14</sub>TAB and C<sub>18</sub>TACl is not the most usual to designate these surfactant molecules, but we believe that it is the most suitable way to identify the length of the hydrocarbon chain.
- [22] D. Wu, A. Chen, C. S. Johnson, *J. Magn. Reson.*, 1995, **115**, 260–264.
- [23] W. S. Price, *Concepts Nucl. Magn. Reson.*, 1998, **10**, 197–237.
- [24] (a) S. K. Mehta, K. K. Bhasin, S. Dham, M. L. Singla, *J. Coll. Interface Sci.*, 2008, **321**, 442–451. (b) R. Lissi, G. Lazzara, S. Milioto, N. Muratore, *J. Phys. Chem. B*, 2003, **107**, 13150–13157. (c) R. Lissi, G. Lazzara, S. Milioto, N. Muratore, I. V. Terekhova, *Langmuir*, 2003, **19**, 7188–7195.
- [25] (a) M. Nilson, C. Cabaleiro-Lago, A. J. M. Valente, O. Soderman, *Langmuir*, 2006, **22**, 8663–8669. (b) C. Cabaleiro-Lago, M. Nilson, O. Soderman, *Langmuir*, 2005, **21**, 11637–11644.
- [26] A. Nakamura, Y. Inoue, *J. Am. Chem. Soc.*, 2003, **125**, 966–972.
- [27] P. Brocos, N. Díaz-Vergara, X. Banquy, S. Pérez-Casas, M. Costas, A. Piñeiro, *J. Phys. Chem. B*, 2010, **114**, 12455–12467.
- [28] (a) W. T. Bentley, R. O. Jones, D. H. Kang, I. S. Koo, *J. Phys. Org. Chem.*, 2009, **22**, 799–806. (b) W. T. Bentley, R. O. Jones, *J. Phys. Org. Chem.*, 2007, **20**, 1093–1101. (c) I. S. Koo, I. Lee, J. Oh, K. Yang, W. T. Bentley, *J. Phys. Org. Chem.*, 1993, **6**, 223–227.
- [29] (a) C. A. Bunton, F. Nome, F. H. Quina, L. S. Romsted, *Acc. Chem. Res.*, 1991, **24**, 357. (b) L. S. Romsted, C. A. Bunton, J. Yao, *Curr. Opin. Colloid Interface Sci.*, 1996, **1**, 514.
- [30] (a) L. Garcia-Rio, J. R. Leis, J. C. Mejuto, J. Pérez-Juste, *J. Phys. Chem. B*, 1998, **102**, 4581–4587. (b) A. R. Alvarez, L. Garcia-Rio, P. Hervés, J. R. Leis, J. C. Mejuto, J. Pérez-Juste, *Langmuir*, 1999, **15**, 8368–8375.
- [31] (a) B. Dorrego, L. Garcia-Rio, P. Hervés, J. R. Leis, J. C. Mejuto, J. Pérez-Juste, *J. Phys. Chem. B*, 2001, **105**, 4912–4920. (b) A. B. Dorrego, L. Garcia-Rio, P. Hervés, J. R. Leis, J. C. Mejuto, J. Pérez-Juste, *Angew. Chem. Int. Ed.*, 2000, **39**, 2945–2948.

## GRAPHICAL ABSTRACT



Multiple recognition by cooperative/competitive mechanisms to form a 1:1:1 inclusion complex plays a crucial role in determining chemical reactivity in the  $\gamma$ -CD cavity.